

PAPER

# Convenient process to synthesize reduced needle platy graphite silver nanocomposite: A prospective antibiotic against common pathogenic microorganisms in the environment

To cite this article: R M N M Rathnayake *et al* 2018 *Mater. Res. Express* **5** 015404

View the [article online](#) for updates and enhancements.

# Materials Research Express



## PAPER

# Convenient process to synthesize reduced needle platy graphite silver nanocomposite: A prospective antibiotic against common pathogenic microorganisms in the environment

RECEIVED  
24 November 2017

REVISED  
26 December 2017

ACCEPTED FOR PUBLICATION  
8 January 2018

PUBLISHED  
24 January 2018

R M N M Rathnayake<sup>1,2</sup> , S K Jayasekara<sup>1</sup>, Hsin H Huang<sup>2</sup>, Masamichi Yoshimura<sup>2</sup>,  
H W M A C Wijayasinghe<sup>1</sup>, R R Ratnayake<sup>1</sup> and H M T G A Pitawala<sup>3</sup>

<sup>1</sup> National Institute of Fundamental Studies, Kandy, Sri Lanka

<sup>2</sup> Graduate School of Engineering, Toyota Technological Institute, 2-12-1 Hisakata, Tempaku, Nagoya 468-8511, Japan

<sup>3</sup> Department of Geology, University of Peradeniya, Peradeniya, Sri Lanka

E-mail: [yoshi@toyota-ti.ac.jp](mailto:yoshi@toyota-ti.ac.jp)

**Keywords:** reduced needle platy graphite, antibacterial properties, silver nanoparticles, *Staphylococcus aureus*, *Pseudomonas aeruginosa*, *Klebsiella pneumoniae*

Supplementary material for this article is available [online](#)

## Abstract

Metal nanoparticles (NPs) have earned keen interest due to differences in their physical and chemical properties according to their size. In this study, reduced needle platy graphite silver (rNPG/Ag) nanocomposite has been prepared using natural vein graphite by *in-situ* chemical reduction method. We found an extraordinary behavior of this rNPG/Ag composite as an antimicrobial agent for pathogenic microorganisms in the environment; *Pseudomonas aeruginosa*, *Klebsiella pneumoniae*, and *Staphylococcus aureus*. Further, above pathogens can build a resistivity against bare silver NPs as well as the rNPG. This is due to the reduction of permeability and enzyme detoxification or efflux of the toxic metal ions. Also, the antibacterial activity of rNPG can be inhibited by poor penetration into the cell as well as the poor dispersion of the material in the medium. On the other hand, the rNPG/Ag composite is used, the Ag nanoparticles embedded with rNPG sheets can enter into the microbial cell through membrane proteins by simple diffusion or endocytosis which inhibits the microbial activity. This penetration of Ag is facilitated by the rNPG sheets as it contributes to the stability and the nano-sized formation of Ag. Our results conduct to develop broad perspective antimicrobial agent using a straightforward and low-cost chemical route.

## 1. Introduction

Recently, extensive efforts have been made to synthesize nanostructures and nanocomposites with different size, shape, crystallinity, and functionality [1–3]. Many of these studies have shown different properties of various forms of carbon and their composites with metals like gold, silver, platinum etc [4, 5]. These carbon-metal composite materials have been fabricated by *in-situ* or *ex-situ* synthesis routine [6–8]. Among these two methods, *in-situ* synthesis is widely reported [9, 10]. The *in-situ* synthesis involves uniform surface coverage of nanocrystals by controlling the nucleation sites on carbon matrices. As a result of that, continuous growth of nanoparticles and their structures on these surfaces can be achieved [4].

The carbon sources used in many studies are based on commercially available graphene materials [11]. The ability to produce graphene oxide (GO) through chemical methods and followed by reduction to produce reduced GO (rGO) directed to the mass production of graphene in solution phase [5, 11]. However, among the different graphite forms, use of natural vein graphite is more beneficial to produce low-cost graphene related products [12]. Among the natural graphite resources all over the world, Sri Lanka has the high-quality vein graphite with high initial purity which has been categorized into four structural varieties [2, 13]. Among those, needle platy graphite (NPG) variety has the highest initial purity such as 99.9% which we used to synthesize

reduced NPG (rNPG). The properties of rNPG can easily be changed by chemical modifications. Recent studies have revealed that the composites of rNPG are in accordance with the environmental remediation [5]. In this regards, the rNPG-silver composite can be used as an antibacterial material for water purification applications and medical applications.

Antimicrobial property of a certain compound is referred to as its ability to kill or suppress the growth of particular microorganisms [14]. These antimicrobial agents can be classified in several ways. For instance, modes of action on microorganism as well as the range of effectiveness are considered to be two specific features in classifications. Also, the range of effectiveness or the spectrum divides antimicrobial compounds into two broad groups as narrow-spectrum (they are effective only against a limited number of pathogens) and broad spectrum (attack many different kinds of pathogens) [15]. Whenever a new antimicrobial compound is discovered, antibiotic susceptibility testing is carried out to determine its effectiveness against different pathogens.

In this study, rNPG/Ag was synthesized using needle platy natural vein graphite (NPG) variety and subsequently used as a possible antimicrobial material [2, 16]. The antibacterial properties of the composite were tested against several pathogens, and we found that the rNPG/Ag composite exhibits antibacterial properties against *Pseudomonas aeruginosa* (ATCC 27853), *Klebsiella pneumoniae*, and *Staphylococcus aureus* (ATCC 25923). Silver is a known antibacterial agent for many microbial pathogens. However, in our study, we found that these pathogens have built a resistivity against bare silver NPs as well as the rNPG. Extracellular or intracellular sequestration of metals, reduction of permeability and alteration of target sites, enzyme detoxification or efflux of the toxic metal ions have been reported as possible mechanisms of pathogens against silver. On the other hand, the antibacterial activity of rNPG can be inhibited due to the poor penetration into cells as well as the dispersion of the material. When the rNPG/Ag composite was added to the medium, the Ag particles are embedded with rNPG sheets which are able to enter into the microbial cell through membrane proteins by simple diffusion or endocytosis and inhibit the microbial activity. This penetration of Ag is facilitated by the rNPG sheets as it contributes to the stability and the smaller size of Ag. Here, we report developing an antimicrobial material with broad spectrum, which can be used against both Gram+ and Gram- pathogens.

## 2. Materials and methods

### 2.1. Materials

For the present study, improved hummers method was used to produce the rNPG followed by the reduction process [2]. NPG variety of Sri Lankan vein graphite was used as the starting material. All the acids (98% H<sub>2</sub>SO<sub>4</sub> and 85% H<sub>3</sub>PO<sub>4</sub>), oxidizing agents (KMnO<sub>4</sub> and 40% H<sub>2</sub>O<sub>2</sub>), silver nitrate, trisodium citrate used for this study were purchased from Sigma-Aldrich.

### 2.2. Preparation of silver nanoparticles

Silver nanoparticles were synthesized using 350 ml AgNO<sub>3</sub> solution of 2 mM concentration. Prepared Ag<sup>+</sup> solution was stirred while heating up to 80 °C for 30 min. Then 70 ml of 10 mM trisodium citrate was added to the mixture drop-wise, with the dropping rate of 0.05 ml s<sup>-1</sup>. Once the whole amount of trisodium citrate was added to the mixture, the mixture was further stirred for another hour. A yellow color solution was observed and this solution was kept to cool down for 6 h.

### 2.3. Preparation of rNPG/silver composite

The details of the synthesis of rNPG using natural NPG vein graphite variety done in our previous work can be found elsewhere [2]. 0.1 g of the synthesized rNPG was sonicated with 350 ml of 2 mM AgNO<sub>3</sub> solution for 30 min. Then the sample was stirred while heating to 80 °C for 30 min and 70 ml of 10 mM trisodium citrate was added to the mixture drop-wise while keeping the dropping rate of 0.05 ml s<sup>-1</sup>. Thereafter the mixture was gently stirred for another 1 h. The prepared composite was kept for 6 h to cool down. After that, the solution was filtered using membrane filter papers and the prepared composite was dried at 60 °C in air for 24 h.

### 2.4. Antibacterial susceptibility testing

The antimicrobial property of rNPG/Ag nanocomposite was tested against six different pathogens using disk diffusion method. Pathogens tested were *Pseudomonas aeruginosa* (ATCC 27853), *Escherichia coli* (ATCC 25922), *Klebsiella pneumoniae*, *Enterococcus faecalis* (ATCC 29212) as Gram negatives and *Staphylococcus aureus* (ATCC 25923), and MRSA-Methylciline resistant *Staphylococcus aureus* as Gram-positive strains. The pathogens were obtained from Department of Microbiology, Medical Faculty, University of Ruhuna, Sri Lanka. These pathogens were separately inoculated into nutrient broth culture medium and incubated at 37 °C overnight. The fully grown cultures were then spread on Muller-Hinton (MH) agar medium to facilitate the diffusion of the

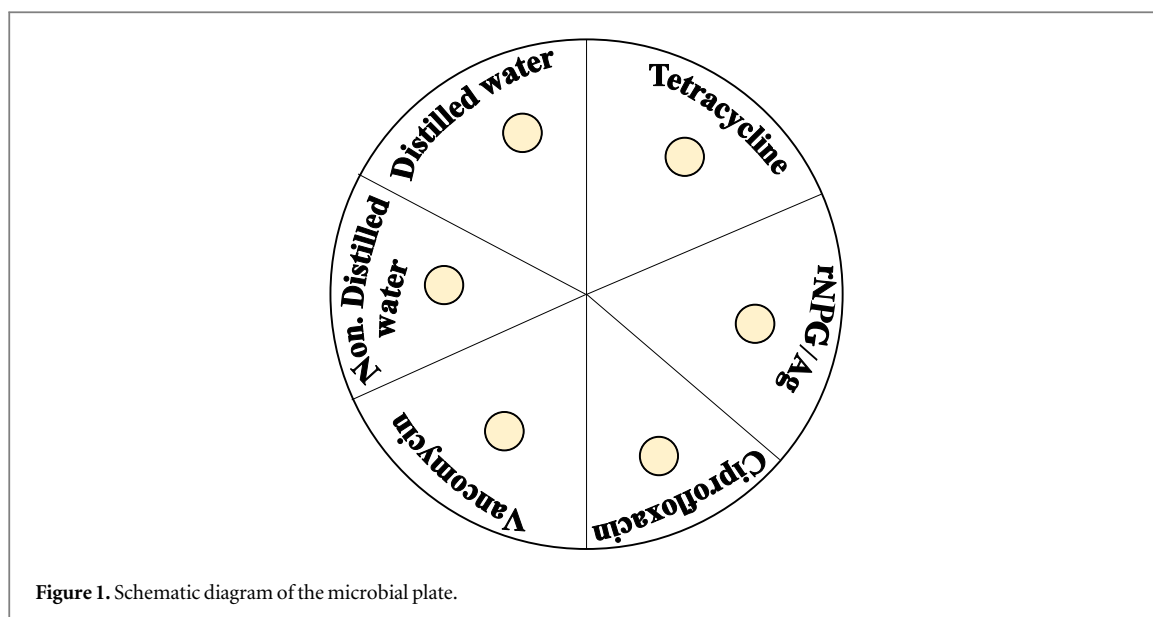


Figure 1. Schematic diagram of the microbial plate.

materials to obtain a successful contact with the pathogens.  $0.02 \text{ g ml}^{-1}$  concentration solutions were prepared for positive controls (Tetracycline, Vancomycin), negative control (Ciprofloxacin) and rNPG/Ag material for the susceptibility testing of the samples. Each material was absorbed to sterilized small filter paper disks (5 mm). These disks were then placed on actively growing pathogenic cultures on MH agar plates. Those plates were incubated at  $37^\circ \text{C}$  for 24 h to observe inhibition zone formation around the disks. The schematic diagram of the plate is shown in figure 1.

### 2.5. Characterization of rNPG/Ag composite

The prepared materials were characterized by x-ray diffraction (XRD) (Rigaku-Ultima IV x-ray diffractometer) with a step size  $0.02^\circ$  and  $\text{Cu K}\alpha 1$  radiation to evaluate the expansion of graphite layers. UV-vis spectroscopic analysis was carried using (Jasco V-650 spectrophotometer) the wavelength range of 200–700 nm. The surface of the samples was studied by scanning electron microscopy (SEM) (HITACHI SU3500). The energy dispersive spectroscopy (EDS) mapping of the samples was obtained by a field-emission SEM (FESEM; HORIBA/X-man, 20 kV). High-resolution transmission electron microscopy (HRTEM) images were obtained by an electron microscope (JEM-2100), operated at an accelerating voltage of 200 kV. Specimens were prepared by dispersing powders in ethanol to form a suspension, and followed by ultrasonication for one hour. The high-resolution images of periodic structures were analyzed and filtered by the fast Fourier transformation (FFT) method. The elemental composition of the material surface was studied by PHI 5000 x-ray photoelectron spectroscopy (XPS) with Al-Mg anode. Raman spectroscopy was carried out to investigate the crystal structure of the prepared expanded graphite samples using Raman Microscope (RENISHAW in-Via) with 532 nm diode laser excitation on  $1800 \text{ lines mm}^{-1}$  grating at room temperature.

## 3. Results and discussion

### 3.1. Material analysis

Reduction of silver ( $\text{Ag}^+$ ) to synthesize silver nanoparticles (Ag NPs) has been achieved using trisodium citrate. rNPG was synthesized using high purity needle platy (NPG) vein graphite [2]. The nanocomposite was synthesized *in-situ* reduction of  $\text{Ag}^+$  with the prepared suspension of rNPG [1]. Though this synthesized material consists of nano-size particles, still they can appear as large particles because of the strong Van der Waal interactions existing between graphene layers and these particles. This would result in the disappearance of the expected properties such as small layer thickness, small particle size expected from rNPG. But this indicates the existence plates like nature of graphite [17]. Interestingly, the yield of rNPG/Ag composite was found to be around 95%. However, compared to the traditional rNPG synthesis methods based on other graphite resources [18].

Figure 2 shows the UV-vis spectrum of Ag, rNPG, and the rNPG/Ag composite material. The selection of the suitable reducing agent and non-toxic stabilizer are essential factors for the stability of Ag NPs because the size of Ag NPs, shape and size distribution is strongly affected by these factors [19]. Metal nanoparticles synthesized by mild reducing agent were relatively more stable than those produced by strong reducing agents

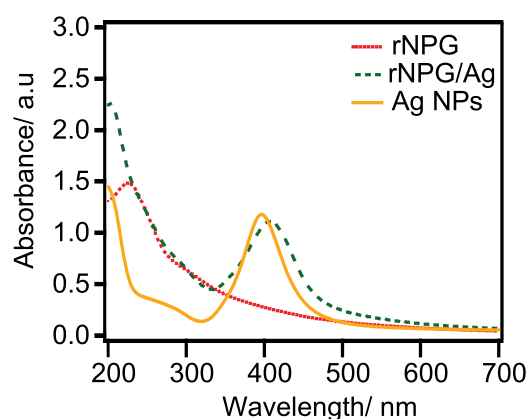


Figure 2. UV-vis spectrum of prepared Ag, rNPG, and rNPG/Ag composite.

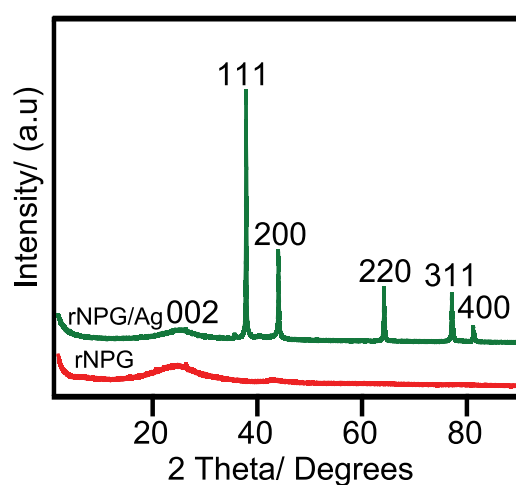
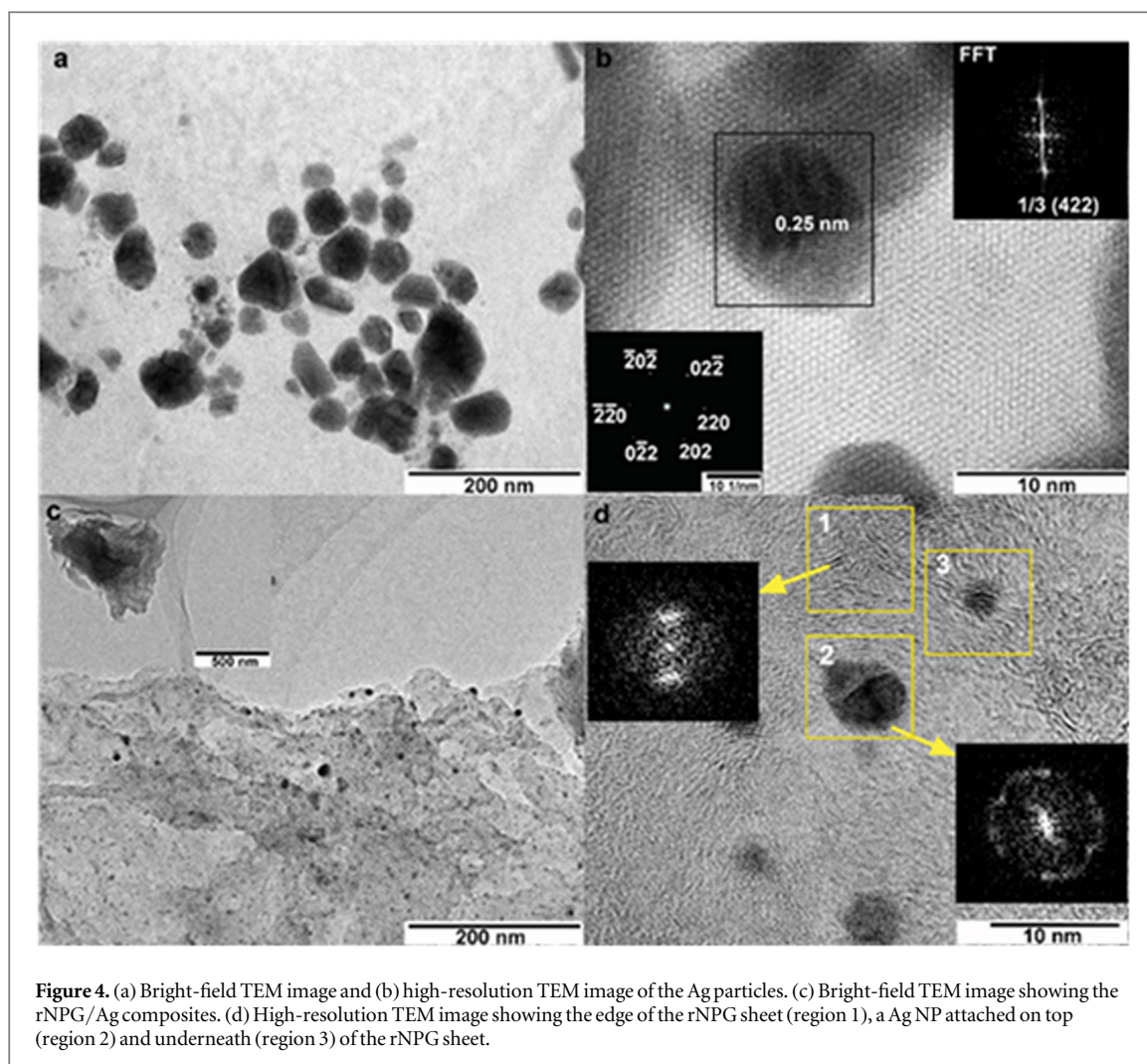


Figure 3. XRD patterns for rNPG and rNPG/Ag composite.

[19, 20]. Trisodium citrate is one of the dual purpose reducing agent, which can also serve as a stabilizing agent. The absorption spectra of the pale yellow silver colloidal showed an absorption band due to surface plasmon resonance with a maximum bandwidth of 402.8 nm indicating roughly spherical Ag NPs particles. This is further confirmed by TEM images shown in figure 4. The position and shape of the plasmon absorption depend on the particle size, shape and the dielectric constant of the surrounding medium [6, 20, 21]. Characteristic peak of rNPG at 245.0 nm indicates the restoration of the extensive conjugated  $sp^2$  carbon network [1, 18, 22]. A new peak is observed after the compositing of Ag NPs with the rNPG; the band at 408.3 nm in the absorption spectrum of rNPG/Ag composite is ascribed to surface plasmon and indicates the presence of Ag NPs [1, 3, 6].

The synthesized rNPG and rNPG/Ag composite were further characterized by using XRD. The XRD patterns of rNPG and rNPG/Ag are shown in figure 3, which confirms the crystalline nature of the rNPG/Ag composite [1, 23]. The diffraction peak at  $2\theta = 25.5^\circ$  ( $d = 0.34$  nm) in rNPG (002) indicates the reduction of NPG vein graphite to rNPG. Though the XRD pattern of rNPG/Ag composite also contains the characteristic peak of rNPG at  $2\theta = 25.6^\circ$ , it is very much reduced. Apart from that, five clear reflections appear in the diffractogram at  $38.04^\circ$ ,  $44.23^\circ$ ,  $64.36^\circ$ ,  $77.31^\circ$  and  $81.35^\circ$  corresponding to the (111), (200), (220), (311) and (400), respectively (JCPD No. 04-0783) [2, 7, 17, 18, 24]. These results of XRD analysis confirm the formation of metallic Ag NPs attached to the rNPG structure. Compared to the XRD pattern of rNPG, the rNPG/Ag composite shows the existing of sharp and strong peaks corresponding to (111) and (200) zone axis of FCC Ag [1, 2, 23]. These results further confirm the preservation of crystallinity in Ag NPs [1, 17].

The size of Ag NPs embedded in the rNPG surfaces was further confirmed by the TEM analysis (figure 4). Interestingly, the Ag NPs distributed on the rNPG surface act as spacers between adjacent rNPG sheets and, a curled and twisted morphology can be observed (figure 4(d)). The Ag NPs are well separated from each other and distributed on the rNPG surface which is further seen in TEM images shown in figure 4. Further, attached Ag NPs may prevent the stacking of the carbon sheets, and therefore the intensity of characteristic diffraction



**Figure 4.** (a) Bright-field TEM image and (b) high-resolution TEM image of the Ag particles. (c) Bright-field TEM image showing the rNPG/Ag composites. (d) High-resolution TEM image showing the edge of the rNPG sheet (region 1), a Ag NP attached on top (region 2) and underneath (region 3) of the rNPG sheet.

peaks of the layered structure was reduced. The XRD pattern of rNPG/Ag nanocomposite shown in figure 3 systematically displays this behavior of Ag NPs with the broadening of the peak at (002) planes of rNPG as are also evident elsewhere [1, 23].

Figure 4(a) depicts the TEM image of Ag nanoparticles, in which the particle size is ranging from 20 to 50 nm. The HRTEM image reveals that the lattice spacing in Ag particle is 0.25 nm (figure 4(a)) corresponding to 1/3 (422) planes of silver [25, 26] confirming the presence of a crystalline silver particle with no secondary phase formed. Moreover, the selected-area electron diffraction pattern was obtained by directing the electron beam perpendicular to one of the spheres. The hexagonal symmetry is shown in the inset of figure 4(b) is indexed to (111) plane of silver, which confirms the high crystalline nature of Ag particles.

As in figure 4(c), the average size of the rNPG particle is 500 nm. After forming the rNPG/Ag composite, it can be seen that almost all the Ag NPs are anchored to the rNPG sheets, indicating a strong interaction between the NPs and the rNPG (figure 4(c)). This can be further confirmed by the HRTEM observation, as shown in figure 4(d). In the region 1, the rNPG edge appears in line contrast with an interlayer spacing of 0.34 nm, which is consistent with the XRD results in figure 3. The corresponding FFT image is indexed to the (002) plane of rNPG. Region 2 is composed of the rNPG sheet with an average size of 10 nm Ag NPs on top of the sheet as shown in figure 4(b). On the other hand, a few NPs are seen to be attached to the underneath of the rNPG sheets, where the rNPG edge contrast is clearly present on top of those Ag particles. Therefore, it is clear that the Ag NPs are firmly attached to the both sides of the rNPG sheets with uniform distribution.

To evaluate the reduction level and to determine the composition of the as-prepared rNPG/Ag composite, XPS analysis was performed. Figure 5 shows the survey spectra obtained on rNPG and rNPG/Ag composite. Further, figures 6–8 represent the de-convoluted C1s spectra of rNPG, de-convoluted C1s spectra of rNPG/Ag composite and de-convoluted Ag<sub>3d<sub>5/2</sub></sub> spectra of rNPG/Ag composite, respectively. The survey spectra of pure rNPG demonstrate the binding energies of 284.4 eV, 398.1 eV and 532.0 eV (figure 5) which are attributed to the C1s, N1s, and O1s bond present in synthesized rNPG, respectively [18]. Further, the same elements are present in the XPS survey spectra of rNPG/Ag composite. This clearly demonstrates that the rNPG synthesized by using

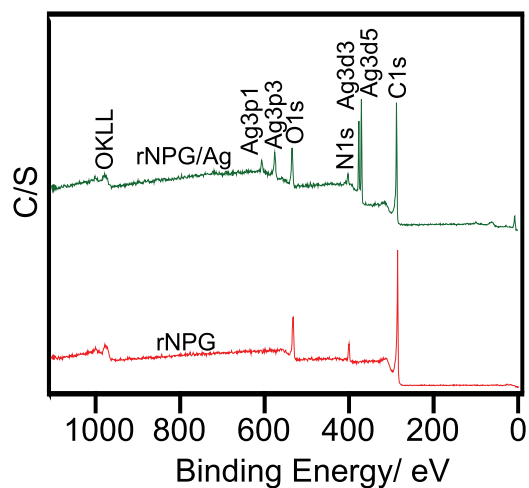


Figure 5. Survey 1s spectra of rNPG and rNPG/Ag composite.

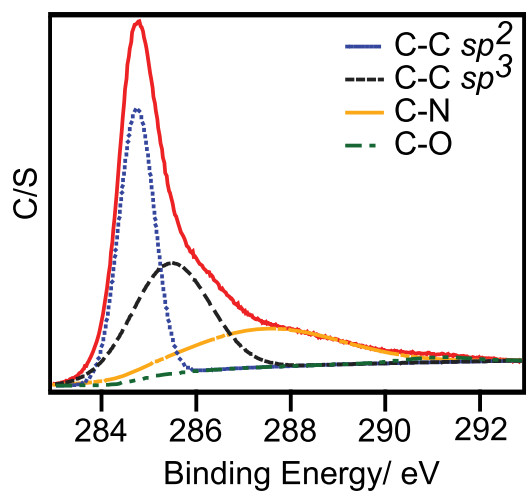


Figure 6. XPS analysis of de-convoluted C1s spectra of rNPG.

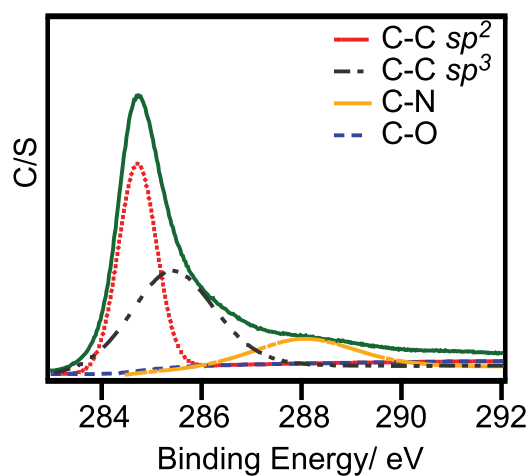
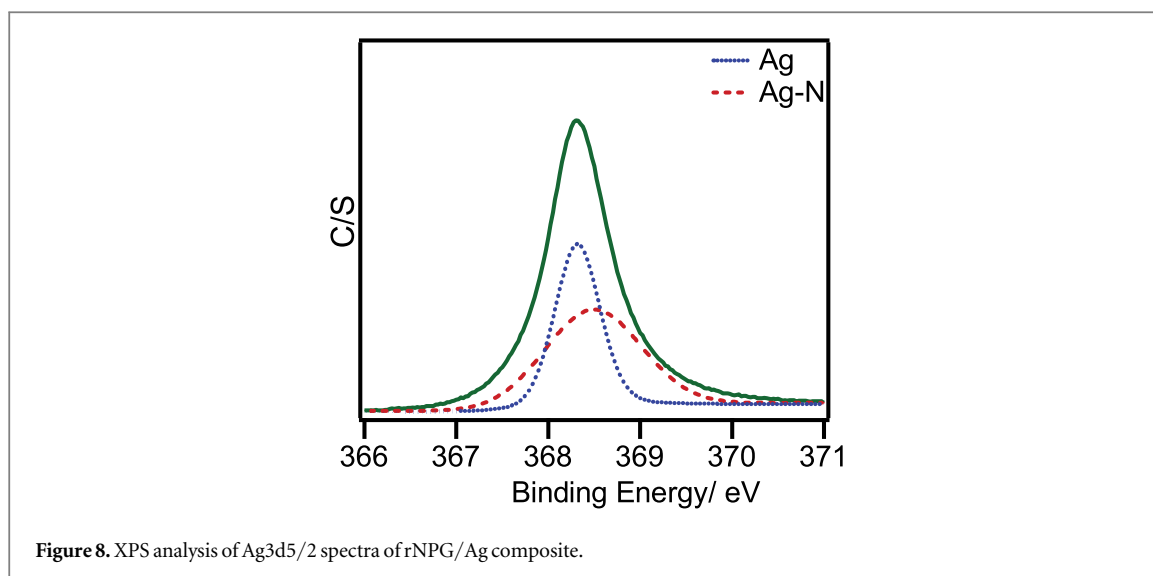


Figure 7. XPS analysis of de-convoluted C1s spectra of rNPG/Ag composite.



NPG vein graphite has not undergone any structural changes during the synthesis [23, 24]. The peaks of 368.04 eV and 374.03 eV present in figure 5 can be attributed to Ag3d<sub>5/2</sub> and Ag 3d<sub>3/2</sub>, respectively [7].

The 5.9 eV splitting of the 3d doublet of Ag directs the formation of metallic Ag on the surface of rNPG [7, 15]. Moreover, the binding energy of 398.1 eV is attributed to N1s of rNPG, which corresponds to the nitrogen atoms from [Ag(NH<sub>3</sub>)]<sup>+</sup> complex. The C1s of rNPG (figure 6) shows four peaks: C–C sp<sup>2</sup> (284.7 eV), C–C sp<sup>3</sup> (285.5 eV), C–N (287.4 eV) and C–O (290.2 eV). The peak position belongs to the C–N bond corresponds to the reducing agent attached with the freshly prepared rNPG [2, 15, 18, 27, 28].

The C1s spectra of rNPG/Ag composite (figure 7) confirms the presence of the same bonding structure of rNPG remaining in the composite after it attached with Ag NPs. The Ag (3d<sub>5/2</sub>) and Ag (3d<sub>3/2</sub>) bands of both samples were found at binding energies of about 368.30 eV and 374.39 eV, respectively. The energy splitting value of 6.09 eV for the 3d doublet of Ag indicates the formation of metallic silver nanoparticles [29, 30]. To further confirm this form of silver, de-convolution of Ag (3d<sub>5/2</sub>) peak (figure 8) was used and it was observed binding energies at 368.3 eV and 368.4 eV which corresponds to the chemical states of Ag<sup>0</sup> and Ag<sup>+</sup> respectively. Further, the formation of these chemical states of the silver is corresponding to the presence of metallic Ag and AgNO<sub>3</sub> in the composite material, respectively. Based on the peak area ratios of the de-convoluted peaks of Ag, more than 70% of silver atoms in the rNPG/Ag composite material were in Ag<sup>0</sup> state, while only about 30% of silvers were in the Ag<sup>+</sup> chemical states. Therefore, the main component of the synthesized Ag nanoparticles dispersed within the rNPG was metallic silver nanoparticles. Further, Ag3d<sub>5/2</sub> spectra of rNPG/Ag composite (figure 8) clearly confirms the presence of metallic Ag NPs combined with the rNPG surface without forming by-products of Ag in excess.

The nitrogen bonds seen in XPS analysis has been disappeared in EDS analysis (figure S3) of the composite material. It may be due to the difference in the detection limits of these two analytical techniques because the XPS can detect significantly low concentrations. In contrast, with the XPS results obtained for atomic nitrogen levels, this EDS indicates the presence of an insignificantly low amount of nitrogen in the composite material.

### 3.2. Antibacterial susceptibility test

The antibacterial susceptibility test has been carried out using six microbes in Gram– and Gram+ groups. Figure 9 shows the results of antibacterial susceptibility test against certain pathogens. Further, figure S2 is available online at [stacks.iop.org/MRX/5/015404/mmedia](https://stacks.iop.org/MRX/5/015404/mmedia) present in supplementary 1 describes the characteristic features of these three pathogens. It was observed that three bacterial strains out of six were sensitive to synthesized rNPG/Ag composite which was done by disk diffusion method. Moreover, the antimicrobial effect of rNPG/Ag composite against these pathogens was further studied by agar well diffusion method and broth culture method (figure S3). It was also observed that *P. aeruginosa* and *K. pneumoniae* were comparatively more sensitive to rNPG/Ag composite and produced maximum growth inhibition zone. Interestingly, rNPG/Ag composite material reports higher antimicrobial properties of this composite material with a broad spectrum of pathogenic species. However, there are some limitations occurred with the dispersion of the suspension to the agar medium [18, 20, 31]. Due to the lack of dispersion of the composite material to the culture medium, broth culture method was used to facilitate the dissolution of the material into the medium and obtained more homogenized distribution of composite (figure S4). The EDX/SEM analysis of broth cultures of each pathogen shows the absence of microorganisms in each broth confirms the inhibitory effect of composite



Figure 9. Optical images of antibacterial susceptibility testing of Gram– and Gram+ pathogens.

Table 1. Antibacterial susceptibility testing results for several test materials.

Organism	Test material					
	Ciprofloxacin	Vancomycin	Tetracycline	rNPG/Ag	Dil. water	None disk
<i>Pseudomonas aeruginosa</i>	+	+	+	+	–	–
<i>Escherichia coli</i>	+	–	+	–	–	–
<i>Staphylococcus aureus</i>	+	+	+	+	–	–
<i>Klebsiella pneumoniae</i>	+	+	+	+	–	–
<i>Enterococcus faecalis</i>	+	–	+	–	–	–
MRSA	+	–	+	–	–	–

Note. (+) positive results, (–) negative results of tested materials for antibacterial susceptibility testing.

material (figures S5, S6, and table S1). Further, we have tested the pH change of the medium when adding the composite material into the culture medium which is a crucial parameter for bacterial growth and results have been demonstrated in table S2.

Moreover, table 1 represents the sensitivity of pathogens to commercially available antibiotics and rNPG/Ag.

After observing the antimicrobial effect of the composite material, it was studied whether this material has ‘cidal’ or static effect against microbial growth. These observations confirm that the material has a static effect which inhibits the microbial growth as illustrated in figure S7.

According to the susceptibility test results, it was observed that three pathogens which showed inhibition against rNPG/Ag composite material were not affected in the presence of bare Ag or rNPG. In other words, although the composite material was inhibitory against selected pathogens, bare silver and rNPG were not.

However, silver is a heavy metal which is considered to be inhibitory against many pathogens over the decades [10]. The antibacterial properties of metallic silver and silver nitrate have been understood in the late 19th century [32–34]. Nevertheless, understanding of mechanisms related to this toxic effect of silver remains incomplete because there are many suggestions that have not been proven. Among the well-known causes of the silver antimicrobial effect, inhibition of respiration, membrane damage and destruction of the proton motive force are profusely discussed.

The interaction of  $\text{Ag}^+$  with thiol groups in membrane proteins/enzymes are thought to be a major mechanism of toxicity, with data suggesting that the key toxicity event is interactions between  $\text{Ag}^+$  and respiratory chain enzymes [35, 36]. It is also found that silver ions and nanoparticles have the ability to cause destabilization of the outer membrane, the collapse of the cytoplasmic membrane potential and depletion of intracellular ATP levels. Another suggestion is that the ability of intracellular silver ions to generate reactive oxygen species under aerobic conditions and interference in DNA replication [37]. There is a consensus that surface binding and damage to membrane function are the most important mechanisms for the killing of bacteria by  $\text{Ag}^+$  [38].

According to the results of the present study, the bare silver solution did not show inhibitory effects against the pathogens used. Presence of metal ion resistant strategies in these microorganisms could be the reason behind this. The potential resistance strategies that they can employ are limited to extracellular or intracellular sequestration of the metal, reduction in permeability, alteration of target sites, enzyme detoxification or efflux of the metal ions [39].

Generally, efflux 'pumping' removes toxic ions that entered into the cell by systems involved in the transport of nutrient cations or oxyanions. Although many resistance mechanisms have been suggested, efflux process is a major as well as currently conceived resistance system. Efflux pumps are transport proteins which participate in the extrusion of toxic compounds out of the cell into exterior environments. These are located in cell membranes of Gram-negative and Gram-positive bacteria. These pumps may be specific for single substance or have the ability to transport multiple numbers of structurally different compounds.

In enzymatic detoxification, toxic metal ions are converted to less toxic or less available metal-ion species [40]. On the other hand, the characteristics of silver particles used in this study may have resulted for the behavior of silver. The size of Ag could be larger than that of the size of Ag attached to the composite material. Therefore, the surface area of Ag around the bacterial cell is considerably low, and hence the Ag density around the bacterial cell is less than that of Ag in the composite material. As a result of that, the feasibility of Ag to pass through the cell wall is declined by preventing the formation of pores in the cell wall structure. As another possibility to initiate this effect caused by Ag could be the stabilization of Ag NPs. Stabilization of Ag NPs obtained using the citrate anion surrounded by the metallic Ag during the reduction process. Further, the microbial cell wall is negatively charged, and therefore, the citrate coated Ag may have repelled by the cell wall. As a result of that Ag may not allow passing through the cell wall into the cytoplasm. This could inhibit the antibiotic activity of bare Ag. One of the mechanisms mentioned above may have resulted in these observations.

When considering the silver nanoparticles, it is believed that they can bind to bacterial cell wall membranes which have slightly negative charge. Then the electron transport between the bacterial cell membrane and the silver nanoparticle can disrupt their wall membranes. On the other hand, silver nanoparticles can interact with thiol groups in proteins, generating reactive oxygen species. Furthermore, replication of the DNA may prevent as a result of the interaction between silver nanoparticles and DNA structure of bacteria. In the present study, silver nanoparticles are embedded in rNPG structure to obtain the rNPG/Ag composite nanomaterial. When silver nanoparticles are embedded in carbon matrices like this, antimicrobial activity depends on the rate of silver release to the bacterial medium. The release of silver in low rates to the medium increases the life efficiency of the antimicrobial activity of composite material while the high rate of silver release into the medium shortens the life efficiency of the antimicrobial activity of the composite material. When nanoparticles are embedded and stabilized in the porous material, the release of silver into the medium can be controlled for a long period of time. To this extent, silver nanoparticles can improve the antimicrobial activity of rNPG as well. In the present study, rNPG/Ag composite material found to be antimicrobial activity against the selected pathogenic microorganisms, *Staphylococcus aureus*, *Pseudomonas aeruginosa* and *Klebsiella pneumoniae* over bare silver and rNPG/Ag material. This proves that the embedding Ag nanoparticles in the rNPG matrix have increased the antimicrobial activity. According to the study discussed in Akhavan *et al*, 2010, *E. coli* has been affected by their composite material. In the present study, *E. coli* was not affected by rNPG/Ag composite. Although the same *E. coli* strain has been studied, this difference may have occurred because the carbon source used and the method of fabricating the composite is different. However, the other Gram-negative strains (*Pseudomonas aeruginosa* and *Klebsiella pneumoniae*) that we have used were positively affected by the rNPG/Ag composite material which needs further studies to prove the mechanism [29].

Furthermore, *Klebsiella pneumoniae*, *Staphylococcus aureus*, and *Pseudomonas aeruginosa*, the microorganisms tested in the experiment may also have general or species-specific resistance mechanisms to silver. According to Percival *et al* (2004), the resistance of the above microorganisms against the biocides like Ag has been documented. However, those mechanisms should be tested and further proved.

rNPG has a thin and planar structure with an average size of 0.50  $\mu\text{m}$  which is little larger than that of the size of the microbial cell structure. Compared to the average size of the microbial cell (0.45  $\mu\text{m}$ ), the particle size of the antibacterial material has to be smaller to allow successful penetration into the cell. On the other hand, size, as well as the dispensability of the material, is strongly affecting the antimicrobial activity. The dispersion of rNPG leads to poor deposition of microbial cells. This can form a weak attraction between the cells and large rNPG particles which can diminish the antibacterial activity [34, 41].

When the composite material is added into the medium, Ag particles which are embedded in rNPG sheets are able to enter into the microbial cell through membrane proteins, simple diffusion or endocytosis. This penetration is facilitated by the rNPG sheets, as it contributes to the stability and the smaller size of Ag. During the formation of Ag NPs in the composite material, rNPG can also be further reduced and form more active sites with sharp edges which can produce active sites in the cell wall to help the access of Ag into the cell. In the present study, it was observed that the rNPG/Ag nanocomposite material has antibacterial activity against *Staphylococcus aureus*, *Pseudomonas aeruginosa*, and *Klebsiella pneumoniae*. Both Gram-positive and two Gram-negative pathogens have been affected by the composite material. However, *E. coli* was not affected by the antimicrobial activity of the rNPG/Ag composite material.

According to Akhavan and Ghaderi (2010) the cell membrane damage due to direct contact with bacterial cells with sharp edges of the nanowalls which is the most probable mechanism of bacterial inactivation that has

been reported in a previous study [30]. *E. coli* being a Gram-negative bacterium with an outer membrane, become more resistant to the cell membrane damage caused by nanomaterial than the Gram-positive *Staphylococcus aureus* which is lacking the outer membrane. In the present study, silver nanoparticles have been embedding using rGO to enhance the antimicrobial activity of silver. When considering the probable mechanism of antimicrobial action, Akhavan and Ghaderi (2010) in the same study have found out that during the contact interaction of bacterial cells with the reduced nanomaterial, it facilitates the better charge transfer between bacteria and more sharpened edges of the reduced nanomaterial. The edges of reduced graphene nanomaterial with extremely high aspect ratio can perform this type of effective direct contact interaction with microorganisms. According to the results obtained in the study by Akhavan and Ghaderi (2010) the reduced oxide nanomaterial was more toxic to both Gram-negative and Gram-positive bacteria while the effect was higher for Gram-positives. This phenomenon was observed in the present study as well. Also, this may damage the cell membrane allowing the internal cellular components to leak out and cause cell death [30].

Another mode of acceleration of the antibacterial activity of this composite material is provided by the development of rNPG aggregates on the cell surface that eventually releases Ag into the cell. The diameter of inhibition zone (DIZ) in disk diffusion test demonstrates the extent of susceptibility to microorganisms. The disk diffusion test results shown in figure 9 clearly explains the diffusion of the composite material in different levels. The strain susceptible to disinfectants exhibits larger DIZ [36, 42, 43]. Further, the disks with rNPG/Ag composite material surrounded by the clear and significantly larger DIZ compared to the disks with bare Ag or rNPG (figure S3). This clearly reveals the embedded Ag ions and/or Ag NPs may be released from the composite powder to the surrounding medium, damaging genetic material in the organisms leading to the inhibited growth of the pathogens [36]. During the susceptibility test, we could obtain a rapid resistivity of the composite material to *Pseudomonas aeruginosa*, *Staphylococcus aureus*, *Klebsiella pneumonia* in higher ratios compared to the other pathogens we used in this study [36, 43].

According to the pH results obtained from the broth culture method (table S2), the pH of the broth mediums of *Pseudomonas aeruginosa* and *Klebsiella pneumonia* obtained with the suspension of the composite material have been slightly decreased. As a result of that, the release of silver ions into the medium could be facilitated due to the change of acidity in the medium. However, drop of the pH value of these mediums is corresponding to the amount of composite material (1  $\mu$ l rNPG/Ag solution was taken from the 0.2 g ml<sup>-1</sup> concentrated initial rNPG/Ag solution) used was very low for each of above culture mediums. Moreover, the culture medium is having a very basic pH level which could not be decreased by the addition of small amount of composite. Because of that, DIZ of above two pathogens has been larger than that of *Staphylococcus aureus*.

After the diffusion of Ag into the cell, it can react with H<sub>2</sub>O<sub>2</sub> released as a result of respiratory reactions in mitochondria in a living cell while converting Ag into Ag<sup>+</sup>. Activation energy which needs for this reaction could be less than the conversion energy required to form H<sub>2</sub>O and O<sub>2</sub> from H<sub>2</sub>O<sub>2</sub> by catalase activity. This released Ag<sup>+</sup> can easily react with macromolecules present in the cell such as proteins and can inhibit the microbial activity. However, the limited conversion of Ag into Ag<sup>+</sup> to the medium allows the regeneration of bacterial pathogens. The above suggested mechanisms for the rNPG and rNPG/Ag must be experimented by further studies in order to confirm the behavior of rNPG/Ag composite against microbial growth.

#### 4. Conclusion

In this study, we found that synthesized rNPG sample was utilized to synthesize rNPG/Ag composite to use as an antimicrobial material against both Gram-negative and Gram-positive pathogens that are known to cause diseases. The prepared suspension out of composite material composed of a homogeneous distribution of Ag NPs. Further, among the tested pathogens, the composite material was more effective on *Pseudomonas aeruginosa* (ATCC 27853), *Klebsiella pneumoniae* and *Staphylococcus aureus* (ATCC 25923). Moreover, distribution of the composite suspension to the medium was very low and therefore, as in commercialized antibiotics; a smooth distribution of the material was not seen. Further, the improvement of homogeneous dissolution of the material in the solution which facilitates its impregnation into the disk may allow the material to exhibit more visible effects.

#### Acknowledgments

This work was supported by the National Institute of Fundamental Studies, Sri Lanka and Graduate School of Engineering, Toyota Technological Institute, Japan.

## ORCID iDs

R M N M Rathnayake  <https://orcid.org/0000-0003-3981-3941>

## References

- [1] Tang J, Chen Q, Xu L, Zhang S, Feng L, Cheng L, Xu H, Liu Z and Peng R 2013 Graphene oxide–silver nanocomposite as a highly effective antibacterial agent with species-specific mechanisms *ACS Appl. Mater. Interfaces* **5** 3867–74
- [2] Rathnayake R M N M, Wijayasinghe H W M A C, Pitawala H M T G A, Yoshimura M and Huang H-H 2017 Synthesis of graphene oxide and reduced graphene oxide by needle plating natural vein graphite *Appl. Surf. Sci.* **393** 309–15
- [3] Huang X, Qi X, Boey F and Zhang H 2012 Graphene-based composites *Chem. Soc. Rev.* **41** 666–86
- [4] Sreepasad T S, Maliyekkal S M, Lisha K P and Pradeep T 2011 Reduced graphene oxide–metal/metal oxide composites: facile synthesis and application in water purification *J. Hazardous Mater.* **186** 921–31
- [5] Gurunathan S, Han J W, Dayem A A, Eppakayala V and Kim J-H 2012 Oxidative stress-mediated antibacterial activity of graphene oxide and reduced graphene oxide in *Pseudomonas aeruginosa* *Int. J. Nanomed.* **7** 5901–14
- [6] Schlögl R and Boehm H P 1983 Influence of crystalline perfection and surface species on the x-ray photoelectron spectra of natural and synthetic graphites *Carbon* **21** 345–58
- [7] Qi X, Wang T, Long Y and Ni J 2015 Synergetic antibacterial activity of reduced graphene oxide and boron doped diamond anode in three dimensional electrochemical oxidation system *Sci. Rep.* **5** 10388
- [8] Dai C, Yang X and Xie H 2011 One-step synthesis of reduced graphite oxide–silver nanocomposite *Mater. Res. Bull.* **46** 2004–8
- [9] Zhu C, Xue J and He J 2009 Controlled *in situ* synthesis of silver nanoparticles in natural cellulose fibers toward highly efficient antimicrobial materials *J. Nanosci. Nanotechnol.* **9** 3067–74
- [10] Lu Z, Xiao J, Wang Y and Meng M 2015 *In situ* synthesis of silver nanoparticles uniformly distributed on polydopamine-coated silk fibers for antibacterial application *J. Colloid Interface Sci.* **452** 8–14
- [11] Zhang C, Lv W, Xie X, Tang D, Liu C and Yang Q-H 2013 Towards low temperature thermal exfoliation of graphite oxide for graphene production *Carbon* **62** 11–24
- [12] Touzain P, Balasooriya N, Bandaranayake K and Descolas-Gros C 2010 Vein graphite from the bogala and Kahatagaha–Kolongaha mines, Sri Lanka: a possible origin *Can. Mineral.* **48** 1373–84
- [13] Sasanka Hewathilake H P T, Karunarathne N, Wijayasinghe A, Balasooriya N W B and Arof A K 2017 Performance of developed natural vein graphite as the anode material of rechargeable lithium ion batteries *Ionics* **23** 1417–22
- [14] Cai X, Lin M, Tan S, Mai W, Zhang Y, Liang Z, Lin Z and Zhang X 2012 The use of polyethyleneimine-modified reduced graphene oxide as a substrate for silver nanoparticles to produce a material with lower cytotoxicity and long-term antibacterial activity *Carbon* **50** 3407–15
- [15] Guzman M, Dille J and Godet S 2012 Synthesis and antibacterial activity of silver nanoparticles against gram-positive and gram-negative bacteria *Nanomed.: Nanotechnol., Biol. Med.* **8** 37–45
- [16] Lu X J and Forssberg E 2002 Preparation of high-purity and low-sulphur graphite from woxna fine graphite concentrate by alkali roasting *Miner. Eng.* **15** 755–7
- [17] Kim J S et al 2007 Antimicrobial effects of silver nanoparticles *Nanomed.: Nanotechnol., Biol. Med.* **3** 95–101
- [18] Kumarasinghe A R, Samaranyake L, Bondino F, Magnano E, Kottegoda N, Carlino E, Ratnayake U N, de Alwis A A P, Karunaratne V and Amaratunga G A J 2013 Self-assembled multilayer graphene oxide membrane and carbon nanotubes synthesized using a rare form of natural graphite *J. Phys. Chem. C* **117** 9507–19
- [19] Dutta S, Ray C, Sarkar S, Pradhan M, Negishi Y and Pal T 2013 Silver nanoparticle decorated reduced graphene oxide (rGO) nanosheet: a platform for SERS based low-level detection of uranyl ion *ACS Appl. Mater. Interfaces* **5** 8724–32
- [20] Naebe M, Wang J, Amini A, Khayyam H, Hameed N, Li L H, Chen Y and Fox B 2014 Mechanical property and structure of covalent functionalised graphene/epoxy nanocomposites *Sci. Rep.* **4** 4375
- [21] Li W-R, Xie X-B, Shi Q-S, Zeng H-Y, Ou-Yang Y-S and Chen Y-B 2010 Antibacterial activity and mechanism of silver nanoparticles on *Escherichia coli* *Appl. Microbiol. Biotechnol.* **85** 1115–22
- [22] Liu S, Zeng T H, Hofmann M, Burcombe E, Wei J, Jiang R, Kong J and Chen Y 2011 Antibacterial activity of graphite, graphite oxide, graphene oxide, and reduced graphene oxide: membrane and oxidative stress *ACS Nano* **5** 6971–80
- [23] Chung D D L 1987 Exfoliation of graphite *J. Mater. Sci.* **22** 4190–8
- [24] Dreyer D R, Park S, Bielawski C W and Ruoff R S 2010 The chemistry of graphene oxide *Chem. Soc. Rev.* **39** 228–40
- [25] Jiao T, Zhao H, Zhou J, Zhang Q, Luo X, Hu J, Peng Q and Yan X 2015 Self-assembly reduced graphene oxide nanosheet hydrogel fabrication by anchorage of chitosan/silver and its potential efficient application toward dye degradation for wastewater treatments *ACS Sustain. Chem. Eng.* **3** 3130–9
- [26] Germain V, Li J, Ingert D, Wang Z L and Pileni M P 2003 Stacking faults in formation of silver nanodisks *J. Phys. Chem. B* **107** 8717–20
- [27] Gao X, Jang J and Nagase S 2010 Hydrazine and thermal reduction of graphene oxide: reaction mechanisms, product structures, and reaction design *J. Phys. Chem. C* **114** 832–42
- [28] Pei S and Cheng H-M 2012 The reduction of graphene oxide *Carbon* **50** 3210–28
- [29] Akhavan O, Abdollah M, Abdi Y and Mohajerzadeh S 2011 Silver nanoparticles within vertically aligned multi-wall carbon nanotubes with open tips for antibacterial purposes *J. Mater. Chem.* **21** 387–93
- [30] Akhavan O and Ghaderi E 2010 Toxicity of graphene and graphene oxide nanowalls against bacteria *ACS Nano* **4** 5731–6
- [31] Das M R, Sarma R K, Saikia R, Kale V S, Shelke M V and Sengupta P 2011 Synthesis of silver nanoparticles in an aqueous suspension of graphene oxide sheets and its antimicrobial activity *Colloids Surf. B* **83** 16–22
- [32] Hobman J L and Crossman L C 2015 Bacterial antimicrobial metal ion resistance *J. Med. Microbiol.* **64** 471–97
- [33] Nanda S S, Yi D K and Kim K 2016 Study of antibacterial mechanism of graphene oxide using Raman spectroscopy *Sci. Rep.* **6** 28443
- [34] Perreault F, de Faria A F, Nejati S and Elimelech M 2015 Antimicrobial properties of graphene oxide nanosheets: why size matters *ACS Nano* **9** 7226–36
- [35] Holt K B and Bard A J 2005 Interaction of Silver(I) Ions with the respiratory chain of *Escherichia coli*: an electrochemical and scanning electrochemical microscopy study of the antimicrobial mechanism of micromolar Ag<sup>+</sup> *Biochemistry* **44** 13214–23
- [36] Bao Q, Zhang D and Qi P 2011 Synthesis and characterization of silver nanoparticle and graphene oxide nanosheet composites as a bactericidal agent for water disinfection *J. Colloid Interface Sci.* **360** 463–70

- [37] Park J, Lee G and Chung J 2009 The PINK1-parkin pathway is involved in the regulation of mitochondrial remodeling process *Biochem. Biophys. Res. Commun.* **378** 518–23
- [38] Percival S L, Bowler P G and Russell D 2005 Bacterial resistance to silver in wound care *J. Hosp. Infection* **60** 1–7
- [39] Hobman J L and Brown N L 1997 Bacterial mercury-resistance genes *Met. Ions Biol. Syst.* **34** 527–68
- [40] Fung M C and Bowen D L 1996 Silver products for medical indications: risk-benefit assessment *J. Toxicol.: Clin. Toxicol.* **34** 119–26
- [41] Panáček A, Kvítek L, Prucek R, Kolář M, Večeřová R, Pizúrová N, Sharma V K, Nevěčná T.j. and Zbořil R 2006 Silver colloid nanoparticles: synthesis, characterization, and their antibacterial activity *J. Phys. Chem. B* **110** 16248–53
- [42] Kawashita M, Toda S, Kim H M, Kokubo T and Masuda N 2003 Preparation of antibacterial silver-doped silica glass microspheres *J. Biomed. Mater. Res. A* **66** 266–74
- [43] Yee M S-L, Khiew P-S, Chiu W S, Tan Y F, Kok Y-Y and Leong C-O 2016 Green synthesis of graphene-silver nanocomposites and its application as a potent marine antifouling agent *Colloids Surf. B* **148** 392–401